ELSEVIER

Biochimica et Biophysica Acta 1457 (2000) 253–262

BIOCHIMICA ET BIOPHYSICA ACTA
BBA

www.elsevier.com/locate/bba

High-field EPR studies of the structure and conformational changes of site-directed spin labeled bacteriorhodopsin

Heinz-Jürgen Steinhoff [a,*], Anton Savitsky [c], Christoph Wegener [a], Matthias Pfeiffer [b], Martin Plato [c], Klaus Möbius [c]

[a] *Lehrstuhl für Biophysik, Ruhr-Universität Bochum, 44780 Bochum, Germany*
[b] *Max-Planck-Institut für Biochemie, Am Klopferspitz 18a, 82152 Martinsried, Germany*
[c] *Institut für Experimentalphysik, Freie Universität Berlin, Arnimallee 14, 14195 Berlin, Germany*

Received 6 July 1999; received in revised form 26 January 2000; accepted 17 February 2000

Abstract

Cw and pulsed high-field EPR (95 GHz, 3.4 T) are performed on site-directed spin labeled bacteriorhodopsin (BR) mutants. The enhanced Zeeman splitting leads to spectra with resolved g-tensor components of the nitroxide spin label. The g_{xx} component shift determined for 10 spin labels located in the cytoplasmic loop region and in the protein interior along the BR proton channel reveals a maximum close to position 46 between the proton donor D96 and the retinal. A plot of g_{xx} versus A_{zz} of the nitrogen discloses grouping of 12 spin labeled sites in protic and aprotic sites. Spin labels at positions 46, 167 and 171 show the aprotic character of the cytoplasmic moiety of the proton channel whereas nitroxides at positions 53, 194 and 129 reveal the protic environment in the extracellular channel. The enhanced sensitivity of high-field EPR with respect to anisotropic reorientational motion of nitroxides allows the characterization of different motional modes for spin labels bound to positions 167 and 170. The motional restriction of the nitroxide at position 167 of the double mutant V167C/D96N is decreased in the M_N photo-intermediate. An outward shift of the cytoplasmic moiety of helix F in the M_N intermediate would account for the high-field EPR results and is in agreement with diffraction and recent X-band EPR data.

Keywords: Electron paramagnetic resonance; Site-directed spin labeling; Retinal protein

1. Introduction

The elucidation of protein motions and related conformational changes is a prerequisite for the understanding of enzymatic processes. The development of new spectroscopic methods which provide high spatial and high time resolution is particularly promising and challenging for biophysical research. In the present approach, W-band (95 GHz) electron paramagnetic resonance (EPR) spectroscopy at high magnetic field (3.4 T) is combined with site-directed spin labeling (SDSL) to study the structure and conformational dynamics of bacteriorhodopsin (BR).

Site-directed mutagenesis has allowed the introduction of nitroxide side chains at almost any desired site in a protein. Recent studies on a large number of spin labeled mutants of the light driven proton pump

* Corresponding author. Fax: +49-234-3214626;
E-mail: hjs@bph.ruhr-uni-bochum.de

0005-2728/00/$ – see front matter
PII: S0005-2728(00)00106-7

BR have shown that the dynamic properties of the nitroxide side chain and thus the EPR spectral line shape contain direct information about the secondary and tertiary structures of the protein in the vicinity of the nitroxide binding site [1–3]. Supplementary data on the protein structure were extracted from the accessibility of the nitroxides for hydrophobic or hydrophilic quenchers and from the polarity of the nitroxide environment [3–5]. Intramolecular distances and their changes upon effector binding were determined from the spin–spin interaction between two or more nitroxides attached to different sites of the protein molecule [6–9].

The development of high-field EPR techniques requiring superconducting magnets has enhanced the Zeeman resolution of rigid-limit spectra of disordered samples from which the principal g-tensor components and their variation due to solute–solvent interactions can be determined with high accuracy [10–12]. The improved sensitivity to local structural influences on spin labels has been used to reveal significant changes in the g-tensor as a function of solvent polarity and chemical structure of nitroxides [13,14]. High-field cw EPR spectra allows a detailed analysis of the anisotropy of the nitroxide motion [15–18]. High-field pulsed EPR with electron spin echo (ESE) detection revealed anisotropic librational motions of semiquinones in photosynthetic reaction centers of *Rhodobacter sphaeroides* [19] and of nitroxides in toluene [20].

The initial goal of the present work was to utilize the high spectral resolution of 95 GHz EPR to refine previous X-band results on the behavior of the magnetic tensors for different nitroxide positions in BR [21]. The enhanced sensitivity of W-band EPR to the matrix polarity in the vicinity of the spin label binding site allows monitoring of the water density in ion channels and its variation upon conformational changes. Additionally, accurate values of the magnetic tensors are a prerequisite for quantitative studies of the nitroxide dynamics which, in turn, provides the data for the structural analysis of the protein [22]. The enhanced sensitivity towards anisotropic motion and librational dynamics is shown to give new information about the dynamics of protein bound nitroxides. These aspects will be discussed with reference to conformational changes of BR induced by photon absorption.

2. Experimental methods

Mutagenesis, expression of BR in *Halobacterium salinarum* and spin labeling with (1-oxyl-2,2,5,5-tetramethylpyroroline-3-methyl)methanthiosulfonate (MTS) was performed as previously described [3]. Glycerol was added to the suspension of membranes in 0.1 M phosphate buffer (pH 6.8), 0.1 M NaCl, to a final concentration of 20 vol% in order to reduce dielectric loss. At this concentration the effect of glycerol on the BR photocycle is small, e.g. the increase of the decay time of the M intermediate amounts to less than 25% [23]. The BR samples were transferred into quartz capillaries with an inner diameter between 0.2 and 0.6 mm. Centrifugation increased the BR concentration to approximately 0.5 mM in the lower part of the capillary.

EPR spectra were recorded with a laboratory-built high-field EPR spectrometer operating at 95 GHz [10,24] equipped with a cylindrical TE011 cavity. A superconducting magnet (Cryomagnetics) provides a maximum field of 6 T. The microwave power is delivered by a 300 mW klystron (Varian) which can be attenuated to optimum values at the cavity. Cw EPR measurements were done with a modulation frequency of 10 kHz and an amplitude of about 0.1 mT. Pulsed measurements were performed with a $\pi/2-\tau-\pi$ pulse echo sequence with the length of the $\pi/2$ pulse adjusted to 80 to 90 ns.

Light induced measurements were performed with a Nd:YAG laser operating at 532 nm. Light was coupled into the cavity by means of a quartz fiber of 0.8 mm diameter. The laser pulsing frequency was generally set to 10 Hz and the output energy was attenuated to 2 mJ providing an energy density at the sample low enough to prevent photobleaching of BR.

3. The polarity of the bacteriorhodopsin proton channel

The sensitivity of the magnetic tensors of nitroxide spin labels towards the polarity of the environment has been used in the past to characterize the behavior of the hydrophobic properties of membranes and proteins [14,21,25]. While the spectral analysis of X-band spectra had to be restricted to extract the

value of the nitrogen hyperfine tensor element A_{zz}, the enhanced resolution of high-field EPR spectra with respect to the g-tensor anisotropy allows additionally the behavior of g_{xx} of nitroxides with very high accuracy to be followed. (We use the conventional molecular axes notation system with the x-axis along the N–O bond and the z-axis perpendicular to the nitroxide ring plane.) The parameter g_{xx} is used here to characterize the hydrophobic barrier the proton has to overcome during its path through BR. The behavior of g_{xx} versus A_{zz} allows classification of the environment of the spin label binding site as protic or aprotic. Single cysteine residues were introduced along the BR proton channel at the positions shown in Fig. 1 using site-directed mutagenesis techniques. The cysteines reacted with the sulfhydryl specific MTS spin label to yield the spin label side chain (R1). Inspection of the photocycle of the spin labeled mutants did not give any evidence for protein unfolding and it was concluded that the overall structure and function of BR is retained [21]. EPR spectra were measured at 200 K to restrict molecular motion. In this temperature regime the dynamics of proteins exhibits glasslike behavior and the reorientational correlation time of an otherwise unrestricted spin label side chain exceeds 100 ns [26], i.e. the nitroxide may be considered as immobilized on the EPR time scale. However, librational motion of a small amplitude may still prevail and be detectable at these temperatures. This will be discussed in Section 6. Examples of spectra are shown in Fig. 2. A powder spectrum simulation with a small component line width is depicted to uncover the hyperfine splittings in the g_{xx} and g_{yy} regions. The experimental spectra exhibit the typical nitroxide powder pattern line shape expected for a dilute distribution of nitroxides. The spectra are clearly resolved into three separate regions corresponding to the components g_{xx}, g_{yy} and g_{zz}. The variation of g_{xx} with the nitroxide binding site is revealed by the shift of the position of the low-field maximum, generally a polar environment shifts g_{xx} to smaller values. g- and A-tensor values were determined from the second derivative of the experimental spectra.

The g_{xx} values for the studied samples are plotted in Fig. 3A as a function of the distance, r, between the nitroxide binding site and the cytoplasmic surface. The distances were measured from the projections of the C_β positions of the respective residue to a line connecting residues R164, the position of which is arbitrarily set to 0 nm, and G73 on the extracellular surface of the protein. An error bar of 0.7 nm indicates the uncertainty of the location of the N–O group (for positions of the respective side chains, cf. Fig. 1). The smallest values of g_{xx} are found for S162R1 and K129R1. These values are slightly smaller than those found for unbound MTS spin label in aqueous glycerol solution, which yields 2.00834. This difference is most likely due to different salt concentrations present in the spin label solution compared to the BR samples. The behavior of g_{xx} reveals a

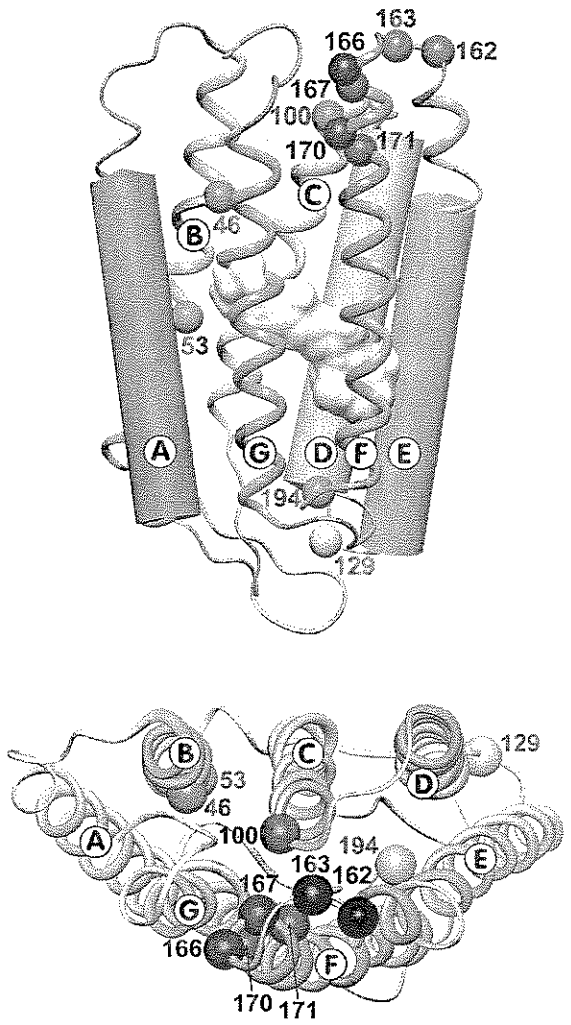

Fig. 1. Structural model of bacteriorhodopsin (BR) with the helices A to G and their interconnecting loops according to the data of Essen et al. [27]. The C_α atom of the spin labeled residues (R1) and the chromophore retinal are indicated.

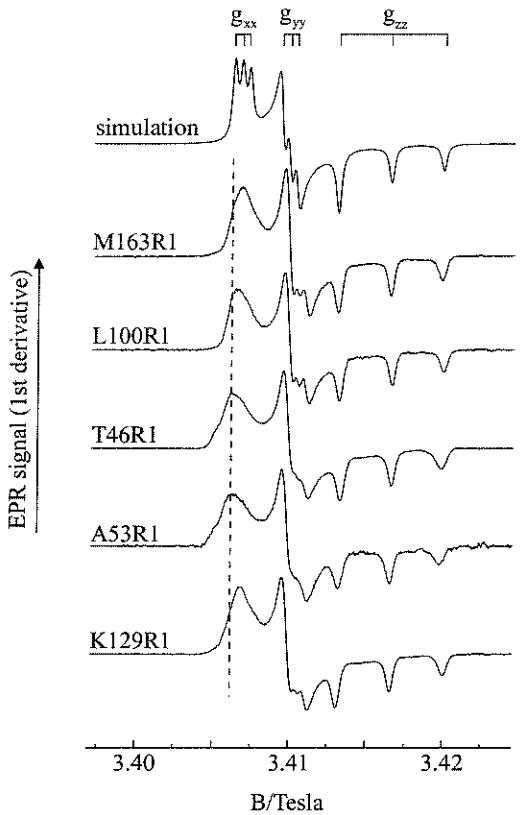

Fig. 2. Experimental high-field EPR spectra (1st derivative representation, $T=200$ K, $\nu=95$ GHz) for a set of spin labeled BR mutants. For comparison the simulation of a powder spectrum is depicted at the top, which was calculated according to the method of Steinhoff and Hubbell [22]. Simulation parameters are $g_{xx}=2.0084$, $g_{yy}=2.0065$, $g_{zz}=2.0025$, $A_{xx}=0.5$ mT, $A_{yy}=0.5$ mT, $A_{zz}=3.41$ mT, $T_2=30$ ns. The vertical line marks the g_{xx} position of T46R1. The variation of g_{xx} reflects the change of polarity in the vicinity of the nitroxide when moving through the BR proton channel from the cytoplasmatic to the extracellular side.

maximum near positions 46 and 53 in the vicinity of the retinal.

The significant variation of g_{xx} with the nitroxide position in BR results from changes in the polarity of the nitroxide environment. According to the molecular model [3,27] residues S162R1 and M163R1 are located in the E–F loop at the cytoplasmic surface, whereas residue K129R1 is positioned in the D–E loop on the extracellular surface. The high polarity in the environment of these residues is clear evidence that the nitroxides are accessible to water, which is in agreement with the structure [28]. The environmental polarity of the nitroxide at positions 100, 167 and 171 is significantly less and reaches its minimum at position 46 between the proton donor D96 and the retinal. The overall behavior of g_{xx} with the varying polarity of the nitroxide environment is consistent with previous results from nitroxides in organic solvents [13]. Earlier measurements of magnetic tensors for different label positions in pure lipid dispersions (dipalmitoylphosphatidylcholine, DPPC) revealed a total variation of g_{xx}, Δg_{xx}, of 6×10^{-4} [14]. The values for g_{xx} found in the present study for the nitroxides located in the proton channel of BR are lower and Δg_{xx} amounts to approximately 3×10^{-4}. Hence, this is evidence for the presence of water or of polar or charged residues in the vicinity of the nitroxides.

It is also very informative to study g_{xx} as a function of the hyperfine tensor component A_{zz} of the N-atom of the nitroxide group. This dependence is plotted in Fig. 3B for the various spin label positions in BR. Obviously, the plot is suggestive of straight-line correlations. Theoretically, both g_{xx} and A_{zz} are expected to be linearly dependent on the π spin density ρ_O at the oxygen atom of the nitroxide group [29–31]. For A_{zz} this is evident from the relation $A_{zz}\propto\rho_N$ and the condition $\rho_N+\rho_O\approx1$. This condition follows from the fact that the spin is practically fully confined to the nitroxide group. For g_{xx}, however, apart from a direct proportionality to ρ_O, there is an additional dependence on specific electronic properties of the oxygen lone-pair orbitals, such as their degree of s, p_x, p_y-hybridization and their orbital energy [29–31]. The lone-pair orbital energy E_n affects g_{xx} via the excitation energy $\Delta E_{n\rightarrow\pi^*}=E_{\pi^*}-E_n$ [32] and is known to be sensitive to a polar environment, e.g. water, and to be particularly sensitive to direct H-bonding of the lone pairs to water or to polar amino acid residues. Such specific environmental effects have been observed experimentally, among others by Kawamura et al. [33] who studied the g_{iso} versus A_{iso} dependence of di-*t*-butyl nitric oxide (DTBNO) in various solvents. They found two different straight lines for aprotic solvents (e.g. *n*-hexane, acetonitrile) and for protic solvents (e.g. methanol, water). These two lines intersect at the point of the least protic solvent *n*-hexane. The values of their slopes, converted to g_{xx} versus A_{zz} for comparison with our data, are -2.9 (aprotic) and -4.4 T^{-1} (protic), respectively. The required conversion of their slopes amounts to an increase by 30%. This correction re-

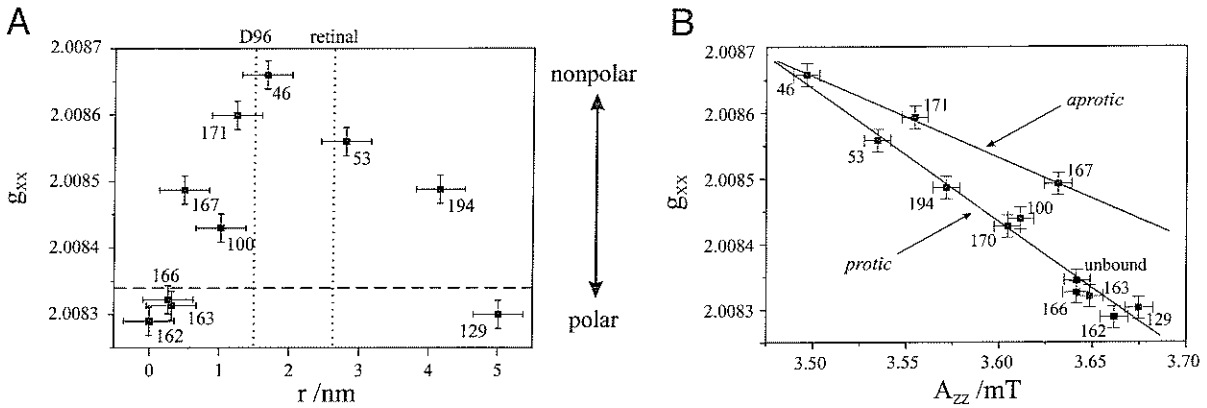

Fig. 3. (A) The tensor element g_{xx} of spin labels oriented towards the aqueous phase or into the proton channel of BR as a function of the nitroxide location with respect to position 164. The horizontal bars indicate the range of the possible locations of the N–O group. Vertical bars (2σ error $\pm 2\times10^{-5}$) are determined by the S/N of the second derivative of the EPR spectra. The broken line shows the g_{xx} value of unbound spin label, the dotted lines indicate the positions of D96 and the Schiff base of retinal, respectively. The value of g_{xx} may be understood as a polarity index, thus the plotted data reflect the hydrophobic barrier in the BR proton channel. (B) Plot of g_{xx} versus A_{zz} of the nitrogen for various spin label positions in BR. The horizontal bars indicate 2σ errors of about $\pm 10^{-2}$ mT for A_{zz}. The vertical error bars are as in (A). For discussion of the straight line dependences, see text.

sults from the following reasoning: the conversion of g_{iso} to g_{xx} is based on MO calculations in our laboratory of the type AMPAC/AM1. They predict practically pure unhybridized p_y-orbitals for the lone-pair electrons. In this case, only g_{xx} is affected, giving $\Delta g_{iso} = (\Delta g_{xx}+\Delta g_{yy}+\Delta g_{zz})/3 = \Delta g_{xx}/3$. The required conversion of A_{iso} to A_{zz} is based on experimental findings for many nitroxides [30,31] which show that A_{zz} is related to A_{iso} by an empirical factor of 2.3. Thus, the overall conversion factor between $\Delta g_{xx}/\Delta A_{zz}$ and $\Delta g_{iso}/\Delta A_{iso}$ amounts to $3.0/2.3 = 1.30$.

We have attempted to establish similar straight-line relations for the various label positions in BR (see Fig. 3B). There are two possible solutions: (I) all points are assembled around one straight line (not shown in Fig. 3B) having a slope of -2.25 T^{-1} with a rather large rms error of ± 0.5 T^{-1}. (II) The points belonging to label positions 46, 171 and 167 on the one hand and all the remaining points on the other hand are assigned to two different straight lines with slopes -1.35 and -2.00 T^{-1}, respectively. Both these slopes have considerably smaller rms errors of ± 0.1 T^{-1} as compared to solution (I).

The proposed grouping of label positions in solution (II) emerges when considering their different environment in terms of numbers of polar residues and water molecules that directly would affect the g_{xx} values [32]. Using INSIGHT II (Biosym) a model of bacteriorhodopsin including adjacent lipids and internal water molecules was built according to the structural data of Luecke et al. [28]. The cytoplasmic and extracellular surfaces were soaked with 5 layers of water molecules. We counted the number N_p of polar residues and internal and external water molecules within a sphere of radius 1 nm around the position of atom C_β of each substituted amino acid residue. A plot of g_{xx} versus N_p shows a significant displacement of positions 46, 171 and 167 towards larger g_{xx} values from the correlation of the remaining positions. We may, therefore, classify these positions as 'aprotic' in the definition of Kawamura et al. [33]. Thus, solution (II) appears to be the preferable sorting procedure as compared to the badly correlated solution (I). We want to mention an interesting alternative to the counting procedure, described above. If simply plotting g_{xx} versus the number N_{np} of nonpolar residues in identical spheres, we obtain the same classification of label positions. This clearly demonstrates the complementary role of these two types of residues.

Solution (II) is also supported by the fact that the ratio of 1.5 of the two slopes coincides with the ratio of the 'protic' and 'aprotic' line slopes in the study of Kawamura et al. [33]. The reduced absolute values of the slopes in our and their studies by a common factor of 2 may be due to diamagnetic shielding in the protein system which is nonexistent in the pure protic or aprotic solvents. It should be pointed out

that the slope of $-1.35\ T^{-1}$ for the 'aprotic' line of solution (II) is close to the slope found for aprotic *n*-PC/DPPC lipid dispersions by Earle et al. [14] for $n \leq 7$ (excluding sterically induced changes of A_{zz} for larger n in the phosphatidylcholine spin labels, *n*-PC, dispersed in the lipid dipalmitoylphosphatidylcholine, DPPC).

The absence of resolved hyperfine structure in the g_{xx} region of the spectra in Fig. 2 suggests that there is a distribution of g_{xx} values, which does not depend on the location of the nitroxide in the proton channel. Ondar et al. [13] have demonstrated that g_{xx} is particularly sensitive to the effect of hydrogen bonding. Thus, the distribution of g_{xx} may reflect hydrogen-bonding interactions with water molecules or amino acid side chains distributed in the proton channel. The existence of a hydrogen bond network within the proton channel has been suggested to facilitate proton conduction between proton donors and acceptors [34] and it was shown that water is required for proton transfer from D96 to the Schiff base [35]. From time-resolved FTIR it was concluded that proton transfer proceeds via an intramolecular hydrogen bond network [36,37]. Neutron and X-ray diffraction studies could localize bound water molecules in the cytoplasmic and extracellular moieties of the proton channel [28,38–40]. According to the structure [28] five polar or charged residues are located in the vicinity of the cytoplasmic proton pathway. On the extracellular pathway up to 10 residues may be involved in a hydrogen bond network. The influence of these residues on the hydrophobic properties is clearly reflected in the behavior of g_{xx} which thus serves as a polarity index of the nitroxide environment. The present results strongly support and expand the polarity data which were extracted from X-band spectra on the basis of the behavior of A_{zz} [21].

4. Analysis of the spin label dynamics

The motion of the nitroxide side chain with respect to the protein backbone results from rotational isomerization about internal bonds of the side chain and the intrinsic flexibility of the backbone. The nitroxide motion is constrained by van der Waals interactions with nearby secondary structures. A nitroxide located in the interior of a protein should reveal high motional restriction due to multiple van der Waals contacts, whereas the dynamics of the nitroxide attached to an isolated helix should be less restricted. Spin label side chains located in loop regions were found to show very high mobility due to additional motional contributions of the flexible backbone. The line width of the center line of X-band EPR spectra, the apparent hyperfine splitting or the second moment of the spectra were used as a qualitative measure which was shown to be correlated with the structure of the binding site environment. The analysis of X-band spectra in terms of the nitroxide dynamics has been proven to be a valuable tool to extract information about the protein secondary and tertiary structure [2,3]. Enhancement of the spectral resolution as in W-band spectroscopy of frozen-solution samples allows relaxation changes in the EPR line shapes to be analyzed in terms of torsional motion of the radicals around different molecular axes, which affects different parts of the spectra. Additionally, high-field EPR line shapes of nitroxide spin probes are sensitive to more rapid reorientational diffusion rates compared to 9 GHz EPR studies. The enhanced resolution of W-band spectra of site-directed spin labeled BR is demonstrated in Fig. 4. The spectra of the spin label side chains at positions 167 and 170 in the cytoplasmic moiety of helix F reflect significant motional constraints. According to the structure (cf. Fig. 1) the nitroxides directly interact with helices C and E, respectively, giving rise to motional restriction. Whereas the X-band spectra of both samples are virtually identical, significant differences are visible in the shapes of the W-band spectra. The EPR absorption of V167R1 corresponding to the orientation of the nitroxide *x*-axis parallel to the magnetic field reveals resolved hyperfine splitting which, however, is smeared out for the g_{yy} region of the signal. The contrary is true for the nitroxide attached to position 170. Spectra simulations according to the method of Steinhoff and Hubbell [22] show that a nitroxide reorientation around the *x*-axis would account for the spectra measured for V167R1. Agreement between simulation and experiment of T170R1 is achieved (not shown) if the reorientation occurs around the nitroxide *y*- or *z*-axis. Thus, W-band spectra clearly reveal differences in the motional anisotropy that is not visible in the

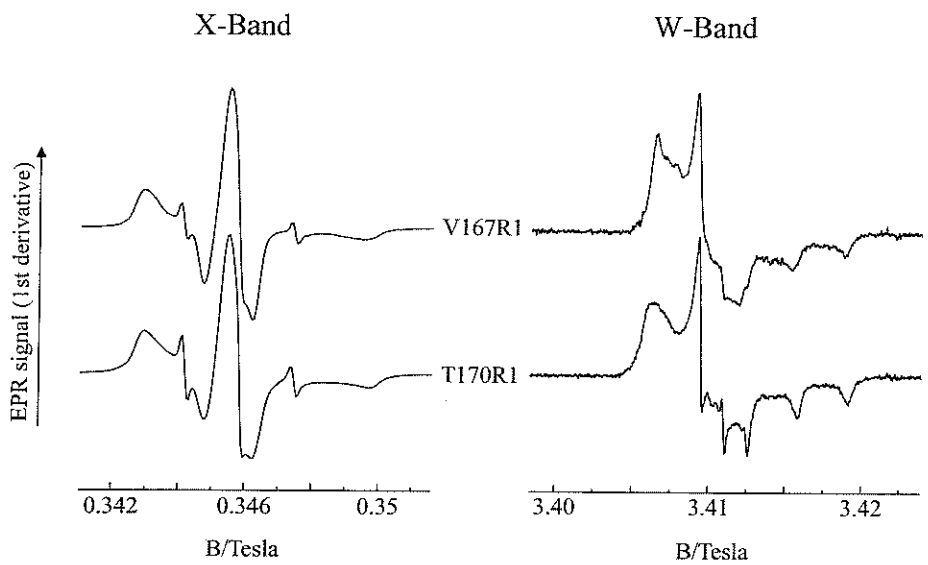

Fig. 4. Left: X-band experimental EPR spectra (1st derivative representation, $T=293$ K, $\nu=9$ GHz) for the spin labeled mutants V167R1 and T170R1 which indicate similar motional restriction. Right: W-band experimental EPR spectra ($T=293$ K, $\nu=95$ GHz) for the same set of mutants. In contrast to the X-band the W-band spectra of both mutants significantly differ and thus reveal different motional restrictions.

corresponding X-band spectra. Molecular dynamic simulations of the nitroxide motion are currently under way to provide a further understanding of the dependence of the motional anisotropy on the structure of the spin label environment. At present, it is easy to appreciate that structural changes in the vicinity of the nitroxide binding site would modulate the motional constraints which in turn change the motional anisotropy. The corresponding spectral changes provide a powerful means of detecting conformational changes in proteins, an example of which is discussed in Section 5.

5. Studies of conformational changes in BR during the photocycle

The sequence of intermediates in the photocycle of BR is associated with significant conformational changes as disclosed by diffraction experiments [41–44] and FTIR spectroscopy [45–47]. The diffraction experiments revealed prominent conformational changes in the vicinity of helix G. A tilt of helix F was reported for BR D96N mutants which was also visible in the frozen wild type to a smaller extent. It is widely agreed that the main structural changes occur during the M intermediate. EPR experiments in combination with site-directed spin labeling provides real time resolution together with specific localization of structural changes. Applying this technique structural changes which influence all of the three cytoplasmic loops and of helix F could be uncovered [48,49]. Interspin distance changes are in agreement with the suggestion of a transient opening of the BR proton channel [7,50]. However, the essence of the conformational change remains still unclear. To elucidate the structural changes in even more detail, experiments with higher resolution in space and time are required.

The enhanced sensitivity of high-field EPR towards the anisotropy of the nitroxide dynamics provides a promising option to describe the influence of conformational changes on the nitroxide motion in the required detail. W-band EPR results on the double mutant V167R1/D96N are shown in Fig. 5. The lack of the proton donor D96 in this mutant leads to a prolonged photocycle which facilitates accumulation of the M intermediate with deprotonated Schiff base at 293 K. This accumulation was achieved by using quasi-continuous illumination with our 532 nm pulsed light source, i.e. by raising the laser repetition rate to values large compared to the M intermediate decay rate. Spectra of the BR initial state were recorded after light adaptation in the dark. Upon qua-

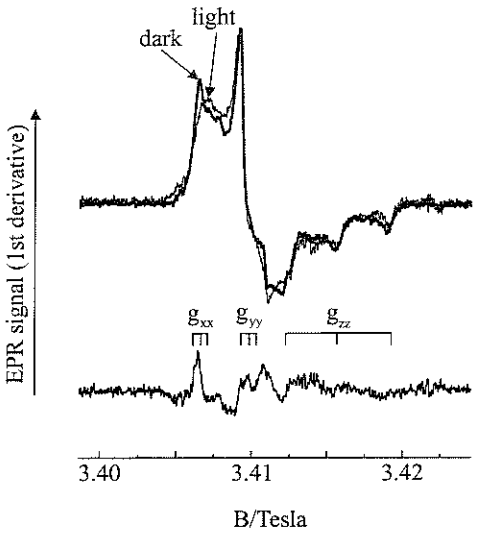

Fig. 5. EPR spectra (1st derivative representation, $T=293$ K, pH 6.8, $\nu=95$ GHz) of the double mutant V167R1/D96N in the dark and in the light. Photo-excitation was achieved with a Nd-YAG laser at $\lambda=532$ nm. The difference dark−light of the two spectra is shown at the bottom. Significant difference amplitudes are observable near the g_{xx} and g_{yy} field regions of the spectrum.

si-continuous light excitation major changes were revealed in the g_{xx} and g_{yy} regions of the spectrum. The observed averaging of the hyperfine splitting in the g_{xx} spectral region and its shift towards the center line is strong evidence for an increased reorientational mobility, at least of the x-axis of the nitroxide in the M intermediate.

The structural change occurs at the cytoplasmic moiety of helix F. The nitroxide side chain of V167R1 is oriented towards helix C [3]. Thus, motion of helix F and/or helix C, which increases the interhelical distance, would weaken the restrictions of the nitroxide mobility and, therefore, would account for the data. These results are in agreement with EPR results on the C–D loop mutant V101R1 [48] and the E–F loop mutant E161R1 [49]. The respective EPR transients revealed structural rearrangements of the E–F and C–D loops that occur during the M intermediate and during the M-to-N transition, respectively, and which reversed with the recovery of the initial state. These results are in agreement with diffraction data which show movements of the cytoplasmic segments of helices B, C and F and a transient ordering of helix G occurring during the M intermediate [42,44,51].

6. Outlook: high-field ESE on site-directed spin labeled BR

In frozen solution, the diffusive residual motion of protein side chains is strongly restricted for temperatures below 200 K. The properties of proteins in this temperature regime have been related to the dynamic glass transition that is well known for glass-forming liquids [52]. Studies using neutron scattering, Mössbauer and EPR spectroscopies have shown that below this temperature mainly vibrational motions are observable [26,52,53]. Above the transition temperature, the motions of fully hydrated samples becomes anharmonic and reveal the character of diffusive motions with larger mean square displacement. A recent study on BR shows that this transition is also observable in the protein–lipid complex of purple membrane in the temperature range between 180 and 220 K [54]. It is of great interest to extend the analysis of the nitroxide motional dynamics below this transition temperature. The objective is to find out whether anisotropic features of the residual librational motion of the nitroxides are observable in BR and to study the dependence on side chain location and protein structure. We started experiments on spin relaxation by high-field electron spin echo (ESE) techniques, which are more sensitive to slow motion characteristics than cw EPR. In Fig. 6, W-band field-swept ESE spectra for sample T170R1,

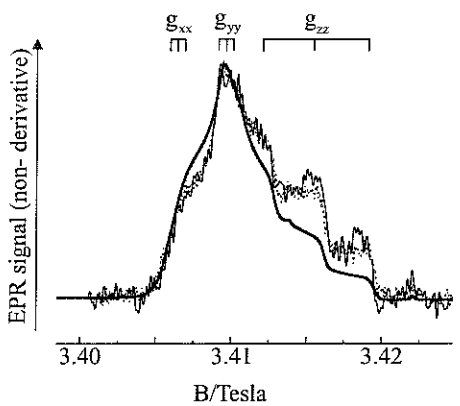

Fig. 6. W-Band (95 GHz) cw (heavy line) and pulsed ESE detected EPR spectra (non-derivative representation) of the mutant T170R1 at $T=170$ K. The pulse sequence was $\pi/2-\tau-\pi$, with τ set to 160 ns (dotted line) and 320 ns (thin line). The behavior of the pulsed spectra close to the canonical positions, g_{xx}, g_{yy}, g_{zz}, indicate stochastic librational motion of the nitroxide side chain. For details, see text.

recorded at 170 K, are shown for two delay times between the pulses in comparison with the non-derivative Boltzmann type cw spectrum. From the different decay behavior of the echo amplitudes of the ESE spectra it is apparent that the T_2 relaxation time is slightly different at different field regions of the spectrum. The relaxation rates at the g_{xx} and g_{yy} spectral positions are larger than at the g_{zz} spectral position, as is indicated by the change in signal amplitudes when recording the spectra for different delay times and for Boltzmann equilibrium. This different relaxation behavior is particularly pronounced in the spectral parts between the canonical peak positions, where any random molecular motion provides large fluctuations of the local field due to large gradients of the resonance frequency. This type of anisotropic relaxation thus provides evidence for anisotropic librational motion [19,55,56]. Additionally, the relaxation due to g-strain fluctuations may contribute, as was shown to be a major effect of relaxation for a highly asymmetric nitroxide spin probe in frozen toluene solution [20]. Further studies on the dependence of the relaxation times on the specific location of the nitroxide label with respect to the protein secondary and tertiary structure are in progress.

7. Conclusion

High-field EPR spectra of site-directed spin labeled BR samples with the label located at the protein surface and in the protein interior were measured below the rigid-limit temperature. The enhanced resolution of W-band high-field EPR spectra provides complete resolution of all canonical peaks of the nitroxide resonance. The value of g_{xx} reflects the polarity of the environment of the nitroxide binding site and allows the hydrophobic barrier of the BR proton channel to be followed. The high Zeeman splitting facilitates in characterizing the spin label site in terms of protic and aprotic environments. The results prove this method to be a valuable tool for future studies of the properties of ion channels. The shape of the hydrophobic barrier in ion pumps and ion channels and its modulation by substrates and conformational changes is subject to intense experimental and theoretical studies. The present study shows the merits of the enhanced g-tensor resolution of 95 GHz EPR spectroscopy for site-directed spin labeling studies on that kind of problems.

Anisotropic reorientational motion of the spin label side chain could be revealed from the analysis of room temperature spectra. Different motional restrictions of nitroxides attached to different locations in the protein emerged from inspection of the high-field EPR spectra in cases, where no differences were detectable in X-band spectra. The analysis of the corresponding spectral features for the double mutant V167R1/D96N at room temperature in the light and in the dark revealed different nitroxide mobilities in the BR photocycle. An opening of the cytoplasmic part of the proton channel during the M intermediate would account for the data. Besides cw high-field EPR also W-band pulse techniques were shown to be applicable to low-temperature studies of anisotropic motion in site-directed spin labeled proteins. They open an exciting new field of investigations of side chain dynamics in proteins. Thus, high-field EPR in combination with site-directed spin labeling has an enormous potential for the study of protein structure and conformational dynamics.

Acknowledgements

We gratefully acknowledge the support of the Deutsche Forschungsgemeinschaft in the frame of the Schwerpunkt-Programm 'Hochfeld-EPR' and SFB 533. We are thankful to A.A. Doubinski (Moscow) and M. Fuhs (FU Berlin) for helpful discussions.

References

[1] C. Altenbach, T. Marti, H.G. Khorana, W.L. Hubbell, Science 248 (1990) 1088–1092.
[2] W.L. Hubbell, H.S. Mchaourab, C. Altenbach, M.A. Lietzow, Structure 4 (1996) 779–783.
[3] M. Pfeiffer, T. Rink, K. Gerwert, D. Oesterhelt, H.J. Steinhoff, J. Mol. Biol. 287 (1999) 163–171.
[4] C. Altenbach, D.A. Greenhalgh, H.G. Khorana, W.L. Hubbell, Proc. Natl. Acad. Sci. USA 91 (1994) 1667–1671.
[5] W.L. Hubbell, C. Altenbach, Curr. Opin. Struct. Biol. 4 (1994) 566–573.
[6] D.L. Farrens, C. Altenbach, K. Yang, W.L. Hubbell, H.G. Khorana, Science 274 (1996) 768–770.

[7] T.E. Thorgeirsson, W.Z. Xiao, L.S. Brown, R. Needleman, J.K. Lanyi, Y.K. Shin, J. Mol. Biol. 273 (1997) 951–957.
[8] H.J. Steinhoff, N. Radzwill, W. Thevis, V. Lenz, D. Brandenburg, A. Antson, G. Dodson, A. Wollmer, Biophys. J. 73 (1997) 3287–3298.
[9] B. Tiebel, N. Radzwill, L.M. Aung-Hilbrich, V. Helbl, H.J. Steinhoff, W. Hillen, J. Mol. Biol. 290 (1999) 229–240.
[10] O. Burghaus, M. Rohrer, T. Götzinger, M. Plato, K. Möbius, Meas. Sci. Technol. 3 (1992) 765–774.
[11] T.F. Prisner, A. Van der Est, R. Bittl, W. Lubitz, D. Stehlik, K. Möbius, Chem. Phys. 194 (1995) 361–370.
[12] M. Huber, J.T. Törring, Chem. Phys. 194 (1995) 379–385.
[13] M.A. Ondar, O.Y. Grinberg, A.A. Doubinskii, Y.S. Lebedev, Sov. J. Chem. Phys. 3 (1985) 781–792.
[14] K.A. Earle, J.K. Moscicki, M. Ge, D.E. Budil, J.H. Freed, Biophys. J. 66 (1994) 1213–1221.
[15] D.E. Budil, K.A. Earle, J.H. Freed, J. Phys. Chem. 97 (1993) 1294–1303.
[16] K.A. Earle, D.E. Budil, J.H. Freed, J. Phys. Chem. 97 (1993) 13289–13297.
[17] T.I. Smirnova, A.I. Smirnov, R.B. Clarkson, R.L. Bedford, J. Phys. Chem. 99 (1995) 9008–9016.
[18] J.P. Barnes, Z. Liang, H. Mchaourab, J.H. Freed, W.L. Hubbell, Biophys. J. 76 (1999) 3298–3306.
[19] M. Rohrer, P. Gast, K. Möbius, T.F. Prisner, Chem. Phys. Lett. 259 (1996) 523–530.
[20] O.G. Poluektov, A.A. Doubinski, Chem. Phys. Lett. 288 (1998) 841–846.
[21] H.J. Steinhoff, M. Pfeiffer, T. Rink, O. Burlon, M. Kurz, J. Riesle, E. Heuberger, K. Gerwert, D. Oesterhelt, Biophys. J. 76 (1999) 2702–2710.
[22] H.J. Steinhoff, W.L. Hubbell, Biophys. J. 71 (1996) 2201–2212.
[23] A.N. Radionov, A.D. Kaulen, FEBS Lett. 387 (1996) 122–126.
[24] T.F. Prisner, M. Rohrer, K. Möbius, Appl. Magn. Reson. 7 (1994) 167–183.
[25] O.H. Griffith, P.J. Dehlinger, S.P. Van, J. Membr. Biol. 15 (1974) 159–192.
[26] H.J. Steinhoff, K. Lieutenant, J. Schlitter, Z. Naturforsch. 44c (1989) 38–46.
[27] L.O. Essen, R. Siegert, W.D. Lehmann, D. Oesterhelt, Proc. Natl. Acad. Sci. USA 95 (1998) 11673–11678.
[28] H. Luecke, H.T. Richter, J.K. Lanyi, Science 280 (1998) 1934–1937.
[29] O. Burghaus, M. Plato, M. Rohrer, K. Möbius, F. MacMillan, W. Lubitz, J. Phys. Chem. 97 (1993) 7639–7647.
[30] M.A. Ondar, O.Y. Grinberg, A.A. Doubinskii, A.F. Shestakov, Y.S. Lebedev, Khim. Fiz. 2 (1983) 54–60.
[31] M.A. Ondar, O.Y. Grinberg, A.A. Doubinskii, Y.S. Lebedev, Khim. Fiz. 3 (1984) 527–536.
[32] A.J. Stone, Proc. R. Soc. London A271 (1963) 424–434.
[33] T. Kawamura, S. Matsunami, T. Yonezawa, Bull. Chem. Soc. Jpn. 40 (1967) 1111–1115.
[34] J. Tittor, C. Soell, D. Oesterhelt, H.J. Butt, E. Bamberg, EMBO J. 8 (1989) 3477–3482.
[35] Y. Cao, G. Varo, M. Chang, B.F. Ni, R. Needleman, J.K. Lanyi, Biochemistry 30 (1991) 10972–10979.
[36] J. le Coutre, J. Tittor, D. Oesterhelt, K. Gerwert, Proc. Natl. Acad. Sci. USA 92 (1995) 4962–4966.
[37] R. Rammelsberg, G. Huhn, M. Lübben, K. Gerwert, Biochemistry 37 (1998) 5001–5009.
[38] T.H. Hauss, G. Papadopoulos, S.A.W. Verclas, G. Büldt, N.A. Dencher, Physica B. 234 (1997) 217–219.
[39] M. Weik, G. Zaccai, N.A. Dencher, D. Oesterhelt, T. Hauss, J. Mol. Biol. 275 (1998) 625–634.
[40] E. Pebay-Peyroula, G. Rummel, J.P. Rosenbusch, E.M. Landau, Science 277 (1997) 1676–1681.
[41] N.A. Dencher, D. Dresselhaus, G. Zaccai, G. Büldt, Proc. Natl. Acad. Sci. USA 86 (1989) 7876–7879.
[42] S. Subramaniam, M. Gerstein, D. Oesterhelt, R. Henderson, EMBO J. 12 (1993) 1–8.
[43] H.J. Sass, I.W. Schachowa, G. Rapp, M.H. Koch, D. Oesterhelt, N.A. Dencher, G. Büldt, EMBO J. 16 (1997) 1484–1491.
[44] S. Subramaniam, I. Lindahl, P. Bullough, A.R. Faruqi, J. Tittor, D. Oesterhelt, L. Brown, J. Lanyi, R. Henderson, J. Mol. Biol. 287 (1999) 145–161.
[45] K.J. Rothschild, M. Zagaeski, W.A. Cantore, Biochem. Biophys. Res. Commun. 103 (1981) 483–489.
[46] K. Gerwert, G. Souvignier, B. Hess, Proc. Natl. Acad. Sci. USA 87 (1990) 9774–9778.
[47] B. Hessling, G. Souvignier, K. Gerwert, Biophys. J. 65 (1993) 1929–1941.
[48] H.J. Steinhoff, R. Mollaaghababa, C. Altenbach, K. Hideg, M. Krebs, H.G. Khorana, W.L. Hubbell, Science 266 (1994) 105–107.
[49] T. Rink, J. Riesle, D. Oesterhelt, K. Gerwert, H.J. Steinhoff, Biophys. J. 73 (1997) 983–993.
[50] N.A. Dencher, J. Heberle, G. Büldt, H.-D. Höltje, M. Höltje, in: A. Pullman, J. Jortner, B. Pullman (Eds.), Membrane Proteins: Structures, Interactions and Models, vol. 25, Kluwer Academic Publishers, Dordrecht, 1992, pp. 69–84.
[51] L.S. Brown, G. Varo, R. Needleman, J.K. Lanyi, Biophys. J. 69 (1995) 2103–2111.
[52] F. Parak, H. Frauenfelder, Physica A 201 (1993) 332–345.
[53] W. Doster, S. Cusack, W. Petry, Nature 337 (1989) 754–756.
[54] J. Fitter, R.E. Lechner, N.A. Dencher, Biophys. J. 73 (1997) 2126–2137.
[55] G.L. Millhauser, J.H. Freed, J. Chem. Phys. 81 (1984) 37–48.
[56] S.A. Dzuba, Yu.D. Tsvetkov, A.G. Maryasov, Chem. Phys. Lett. 188 (1992) 3–4.